Synthesis and characterization of Al-Y co-doped ZnO powders with high photocatalytic properties

JIA HONG ZHENG[a,b,*], SHI FENG NIU[c], RUO YAO ZHENG[a], WEN XUE ZHANG[a], PENG FEI YU[a]
[a] *School of Materials Science and Engineering, Chang'an University, Xi'an 710064, P. R. China*
[b] *Key Laboratory of Preparation and Applications of Environmental Friendly Materials, Ministry of Education, Jilin Normal University, Siping 136000, P. R. China*
[c] *College Key laboratory automotive transportaion safety technology ministry of communication, chang'an university, xi'an, 710064, P. R. China*

A series of $Zn_{0.93-x}Y_{0.07}Al_xO$ samples has been synthesized by the sol–gel method. The structural, optical and photocatalytic properties of the samples were investigated by X-ray diffraction (XRD), energy dispersive X-ray spectroscopy (EDX), X-ray photoelectron spectroscopy (XPS), UV-visible Spectroscopy (UV-Vis). The XRD results showed that all diffraction peaks corresponded to wurtzite structure of ZnO, the doping did not change the structure of ZnO. The values of crystallite particle size and lattice constant of c decrease with the increasing Al doping concentration. EDX measurements showed that Al and Y co-doped ZnO nanoparticles are made of Zn, O, Y, and Al. The photocatalytic activities results indicated that the increase of Al content from 1 to 15 at mol% effectively increased the degradation efficiency. The doping concentration of of 15at% of aluminum in the Al-Y co-doped ZnO is ideal for use in photocatalyst, which degraded almost all the dye (about a 100%) in only 20 min.

(Received October 9, 2014; accepted April 5, 2016)

Keywords: Semiconductor, Al-Y co-doped ZnO; ZnO film, Photocatalytic properties

1. Introduction

The important role of morphology related properties of nanostructures has stimulated tremendous efforts in the design and synthesis of nano-materials with special dimension, morphology and sizes [1-3]. Low-dimensional nano-materials provide an approach to study the fundamental roles of dimensionality and quantum size effect and their application in electronic, optical and piezoelectric devices [4-8].

Among low-dimensional nano-materials, zinc oxide (ZnO) is a widely studied material because it is inexpensive and nontoxic with remarkable optical property. ZnO, which crystallized in hexagonal wurtzite structure, is a wide band gap and n-type semiconductor with a direct optical band gap of 3.37 eV and large exciton binding energy of 60 meV [9], which is very suitable candidate for a wide range of applications such as light emitting diodes [10], dye sensitized solar cells [11], sensors [12], and transparent conductive electrodes [13].

Moreover, ZnO also can be used as a kind of photocatalyst to decompose organic pollutants in air or water under the excitation of UV light. Among these investigations, many researchers reported that the photocatalytic efficiency could be significantly improved in nanomaterials by doping. Doped ZnO powders revealed electrical conductivity similar to that of indium tin oxide (ITO); however, they take more advantages than ITO due to the fact that the ZnO is nontoxicity, pollution-free, thermally stable and is at a lower cost to the manufacture. A number of researches demonstrated that ZnO powders doped with different ions exhibit both lower resistivity and higher transmittance in the visible region. These properties make them ideal for use in photocatalyst. Among these dopants, it was found that the presence of a small quantity of Al can effectively improve the photocatalytic activity of ZnO during the degradation of organic pollutants. However, up to the author's knowledge, Al and Y co-doped ZnO nanomaterials has not yet been studied as a photocatalyst.

In our previous work, we have investigated the effect of Y-doping and Al-doping on the optical properties in ZnO samples [14, 15]. In this work, we reported the room temperature photocatalyst properties of $Zn_{0.93-x}Y_{0.07}Al_xO$ powders prepared by the sol–gel method. Most of the studies concerning the photodegradation of organic compounds using ZnO have been carried out with suspensions of fine powdered ZnO in aqueous solutions [16-18]. The use of fine powders increases the photocatalytic efficiency due to the high effective surface area of the material. The sol–gel method is a good to synthesize powders. This sol–gel method allows the mixing of the chemicals at the atomic level, thus the possibility of forming an undetectable impurity phase could be reduced. Hence, the physical properties of the samples prepared by this method usually exhibit their intrinsic nature. The sol–gel method also has other advantages such as good reproducibility and a simple experimental procedure [19, 20]. The effect of Al on the

structure, optical and photocatalyst properties of ZnYO has been studied in detail.

2. Experimental

2.1 Sample preparation

$Zn_{0.93-x}Y_{0.07}Al_xO$ powders with x = 0.00, 0.03, 0.05, 0.07, 0.11, 0.13 and 0.15 at% were prepared via the sol–gel method. All the chemical reagents used in the experiment were analytical grade purity. Zinc nitrate [$Zn(NO_3)_2 \cdot 6H_2O$] and different ratios of yttrium nitrate [$Y(NO_3)_3 \cdot 6H_2O$] and aluminum nitrate [$Al(NO_3)_3 \cdot 9H_2O$] were dissolved into the citrate acid [$C_6H_8O_7 \cdot H_2O$] solution with stirring to form the sol. Then, the mixture was polymerized to form gel at 80 °C. The swelled gel was pyrolyzed at 130 °C to obtain the reticular precursor. The precursor was further ground into powders in an agate mortar and then sintered at 450 °C for 3 h in a tube furnace with Ar atmosphere as the carrying gas to obtain $Zn_{0.93-x}Y_{0.07}Al_xO$ powders.

2.2 Characterisation techniques

X-ray diffraction was employed to determine the phase structure, performed on a D/max-Rigaku XRD diffraction spectrometer with a Cu Kα line of 1.5417 Å and a monochromator at 50 kV and 300 mA. The compositional analysis of synthesized samples was carried out using energy dispersive X-ray spectroscopy (EDX). The photocatalytic activities of the products were evaluated by the degradation of methyl orange aqueous solution, which is one of model organic pollutants. Typically, the ZnO samples were put in the 50 ml aqueous solution containing 20 mg/L methyl orange. Before irradiation, the solution was putted in the dark for 30 min to ensure the establishment of an adsorption-desorption equilibrium between the photocatalysts and the MO aqueous solution. Then the reactors were irradiated for different time with sunlight. After irradiation the methyl orange was analyzed by using UV-visible Spectroscopy (725 PC). Following the exposure to light, the degradation of methyl orange at its absorption maximum (464 nm) was recorded as a function of time.

3. Results and discussion

The crystal structure and phase of the fabricated samples was analyzed through X-ray diffraction (XRD) pattern and resultant pattern was shown in Fig. 1. XRD measurements were taken from 20 degree to 80 degree with a 0.02 degree step size. Fig. 1 shows typical XRD patterns of Al-Y co-doped ZnO powders with different Al doping concentration. A comparison with the standard card demonstrates that the positions of the diffraction peaks can be indexed to know the hexagonal wurtzite structure of ZnO and matched with JCPDF card: No 36-1451, indicating the doping did not change the structure of ZnO. Moreover, no significant peaks for metal aluminum, yttrium, aluminum oxide, and yttrium oxide were observed, indicating that the as-synthesized powders exhibited a hexagonal wurtzite structure. The crystallite particle sizes of Al-Y co-doped ZnO samples were determined from X-ray diffraction data. The crystallite grain size D can be estimated using the Scherrer Formula [21]

$$D = \frac{0.9\lambda}{\beta \cos\theta} \tag{1}$$

where λ is the X-ray wavelength, θ is the Bragg diffraction angle, β is the FWHM in radians. Crystalline particle sizes of the six samples are 34.2, 33.8, 32.3, 31.1, 28.9, 26.2, 24.6 and 22.2 nm. The values of crystallite particle sizes decrease with the increasing Al doping concentration, which is the result of surface reaction competition [22]. Al-O bond energy is higher than Zn-O bond energy, the reaction mobility to raise growth surface will decrease with increasing doping concentration.

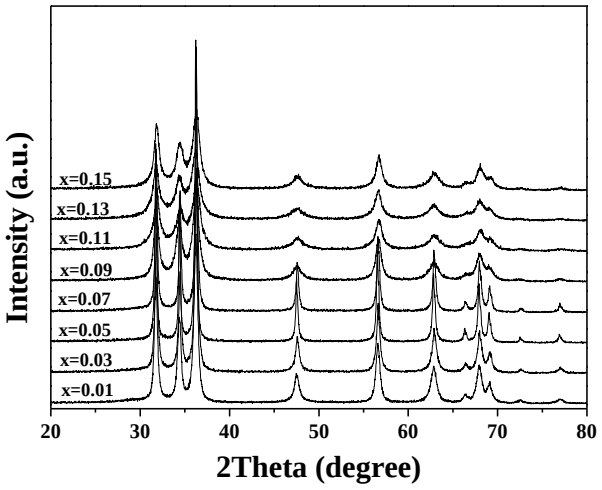

Fig. 1. X-ray diffraction spectra of $Zn_{0.93-x}Y_{0.07}Al_xO$ nanoparticles.

The crystal lattice constant c and the interplanar distances of the diffracting planes d were identified using the Bragg equation $n\lambda = 2d\sin\theta$, where n is the order of the diffracted beam, λ is the wavelength of the X-ray and θ is the angle between the incoming X-ray and the normal of the diffracting planes. Fig. 2 shows the variation of lattice parameters c of thus-obtained $Zn_{0.93-x}Y_{0.07}Al_xO$ as a function of Al^{3+} doping content. It can be seen from Fig. 2 that the lattice parameters c of $Zn_{0.93-x}Y_{0.07}Al_xO$ decreases monotonically with the increase of Al^{3+} Doping content. This may result from the difference of ionic radius of Al^{3+} (0.053 nm) and Zn^{2+} (0.074 nm) ions. Fig. 3 shows the interplanar distances of the diffracting planes d decreased with increasing of doping. This is due to the smaller ionic

bond radius of Al-O than that of Zn-O [23]. This indicates an increase in lattice strain [24].

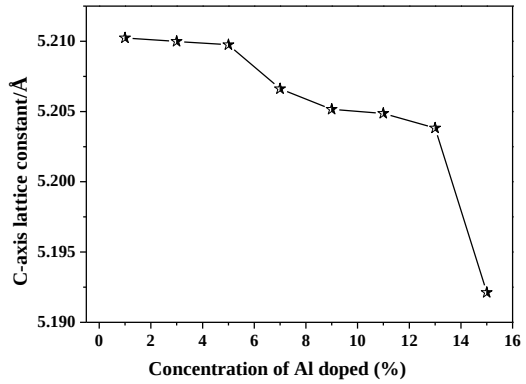

Fig. 2. The variation of c-axis lattice constant of $Zn_{0.93-x}Y_{0.07}Al_xO$ nanoparticles as a function of Al^{3+} doping content.

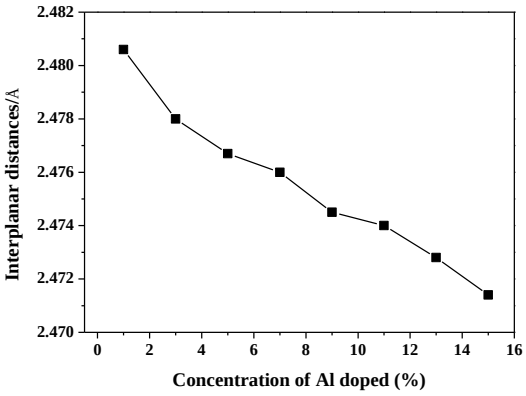

Fig. 3. The variation of interplanar distances of $Zn_{0.93-x}Y_{0.07}Al_xO$ nanoparticles as a function of Al^{3+} doping content.

Valenzuela et al. reported that the full-width at half maximum (FWHM) of an XRD peak is dependent on the crystallite size and the lattice strain caused by the defect and/or dislocations [25]. Fig. 4 shows the FWHM of the diffraction (002) peak of the $Zn_{0.93-x}Y_{0.07}Al_xO$ powders with increasing Al at%. The crystalline size decreased make mention of above but the FWHM increased with increasing Al at%, which means that a high Al doping concentration deteriorated the crystallization quality of the $Zn_{0.93-x}Y_{0.07}Al_xO$ powders, as evidenced by the decrease in intensity of peak in Fig. 1. This phenomenon relates to the positioning behavior of doping atoms in the crystal structure of ZnO. Almost all doping atoms may substitute with the Zn atoms in low Al content. Since the amount of Al is low and their ionic radii are too close to that of ionic radius of Al^{3+} (0.053 nm) and Zn^{2+} (0.074 nm) ions [26], the ZnO crystal structure does not distort severely. The ZnO hexagonal wurtzie structure and substitutional positioning process on ZnO lattice is schematically shown in Fig. 5.

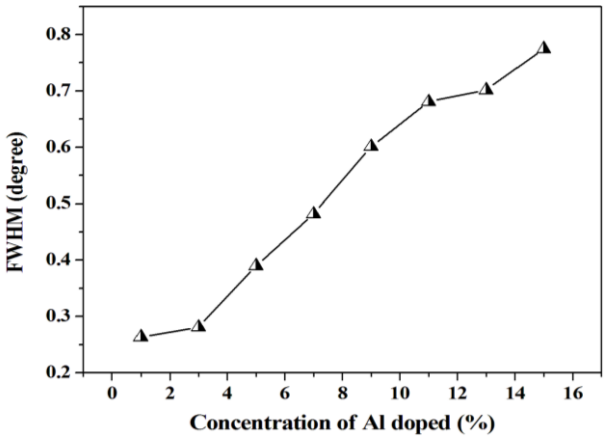

Fig. 4. The FWHM and grain size of the $Zn_{0.93-x}Y_{0.07}Al_xO$ nanoparticles with various Al doping contents.

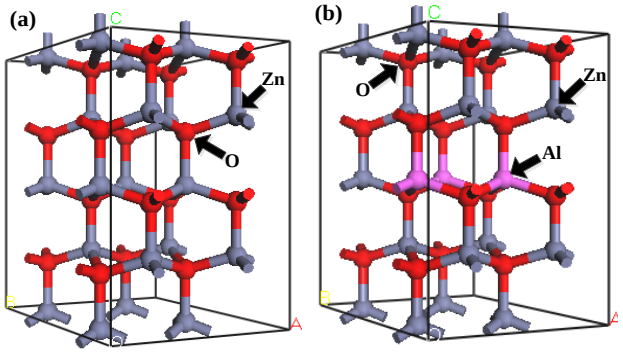

Fig. 5. Schematic representation of (a) ZnO hexagonal wurtzie structure, (b) substitutional doping Al atoms in ZnO.

To assess the elemental composition of the synthesized AYZO powders, the chemical compositions of the as-prepared nanostructures were analyzed by energy-dispersive X-ray spectroscopy (EDX). The corresponding EDX spectra of dual doped ZnO nanostructures taken in the SEM mode are shown in Fig. 6. In EDX spectrum, numerous well-defined peaks were evident concerned to Zn, O, Y, and Al which clearly support that the AYZO nanoparticles are made of Zn, O, Y, and Al. No other peaks related to impurities were detected in the spectrum, which further confirms that the synthesized nanoparticles are the phase-purity of the sample. The observed percentage of Y, Zn and Al values matches well with the amounts of Y, Zn and Al used in the respective precursors without any other characteristic peaks. The analysis proves the fact that sol-gel method is very effective as no loss of elements occurred during the synthesis.

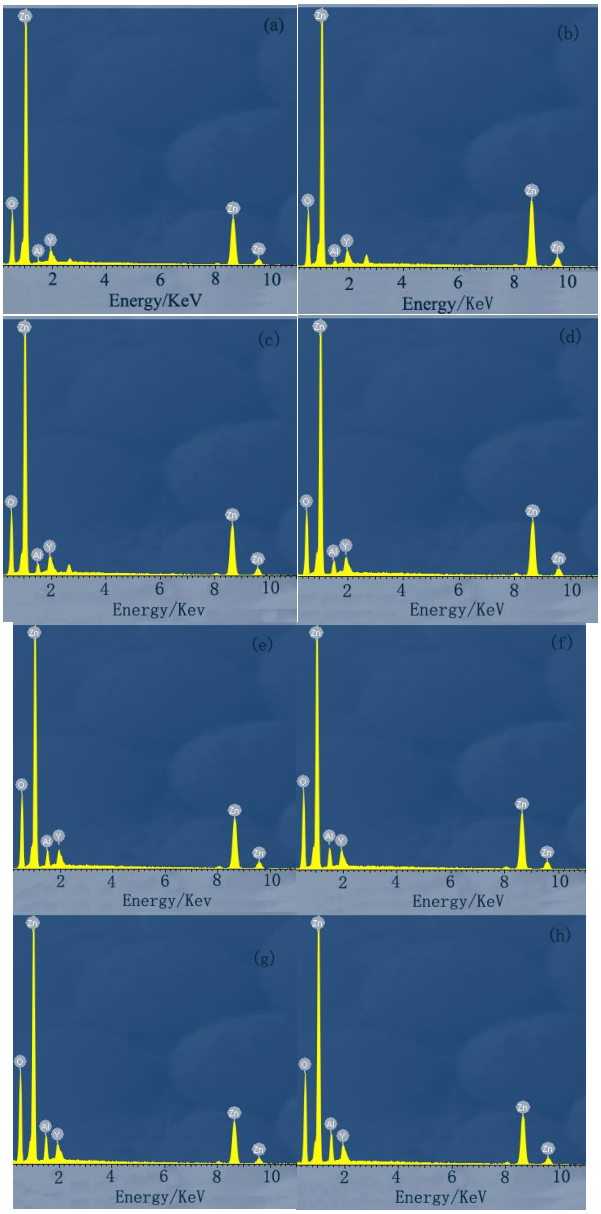

Fig. 6. EDS images of Y–Al codoped ZnO films with different Al concentration: (a) 1 at%, (b) 3 at %, (c)5 at%, (d) 7 at %, (e) 9 at%, (f) 11 at%, (g) 13 at%, and (h) 15 at%

The catalyst's lifetime is an important problem in the photocatalytic degradation, so it is necessary to evaluate the stability and recyclability of the catalyst for practical application. The photocatalytic activities of the samples were evaluated by measuring the decomposition of methyl orange in an aqueous solution under ultraviolet light and sunlight irradiation. The degradation of the methyl orange dye was measured by following the evolution of the intensity of the absorption band centered at 465 nm, as a function of the illumination time, as it is shown in Fig. 7. Fig. 7 shows an example of the absorption spectra evolution as a function of the illumination time in the presence of 5 at.% Al–$Zn_{0.93-x}Y_{0.07}Al_xO$ catalyst. Before the photocatalytic experiment, the suspension solutions of MO-AYZO catalyst were kept in the dark for 60 min to reach an adsorption/desorption equilibrium. The UV–vis absorption spectra of MO (Fig. 7) dye solutions show that the characteristic absorption of MO decreases rapidly with the increase of irradiation time.

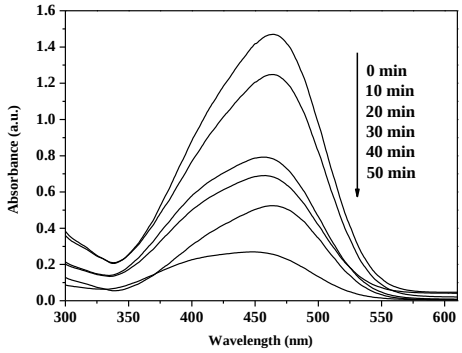

Fig. 7. Evolution of the absorption spectra of MO dye with the illumination time in the presence of 5 at.% Al–$Zn_{0.93-x}Y_{0.07}Al_xO$ catalyst.

After 30 min of sunlight irradiation, the photocatalytic degradation percentage of MO dye with different photocatalysts was calculated by the equation:

$$\text{Degradation \%} = (1-\frac{A_0}{A})\times 100\% \qquad (2)$$

where, A_0 is the equilibrium absorbance of dye at the adsorption/desorption equilibrium state in the absence of sunlight, and A is the absorbance of MO aqueous solution after sunlight irradiation.

Fig. 8 shows the effects of Al doping content on the photocatalytic activity. As it is appreciated in Fig. 8, the Al-Y co-doped ZnO powders degraded almost all the dye (about a 100%) in only 20-50 min, while the undoped ZnO powders reached the same value after almost 3h of illumination (not shown). It is clearly seen that the presence of 15at% of aluminum in the Al-Y co-doped ZnO matrix accelerates the photocatalytic process. It is also appreciated in Fig. 8, the increase of Al content from 1 to 15 at. % effectively increased the degradation efficiency.

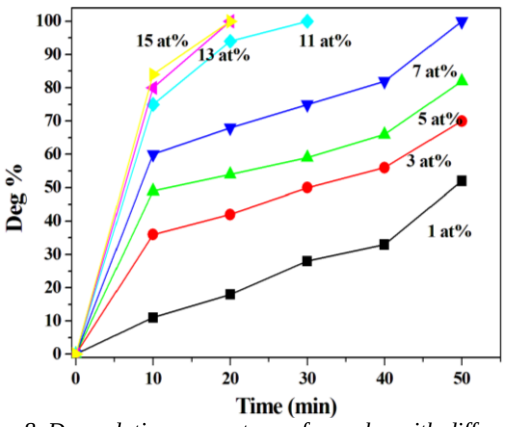

Fig. 8. Degradation percentage of samples with different aluminum concentration

The kinetics of the reaction was obtained by plotting the natural logarithm of the concentration ratios (ln A_0/A) versus the irradiation time. Straight lines were obtained, indicating that the reactions are of first order. It is clear in Fig. 9 that the increment in aluminum concentration gives a better photocatalytic response. To quantitatively understand the reaction kinetics of the MO degradation in our experiments, we used a pseudo-first order model for low dye concentrations:

$$\ln (A_0/A) = k \times t \quad (3)$$

A_0 and A are the concentrations of dye in the aqueous solution at time t=0 and t respectively, and k is the pseudo-first order rate constant. The rate constants obtained from the equation ln (A_0/A) vs t are plotted in Fig. 10. As it is shown in Fig. 10, the sample of 15% Al doped concentration with the highest rate, giving a k = 13.8 h^{-1}.

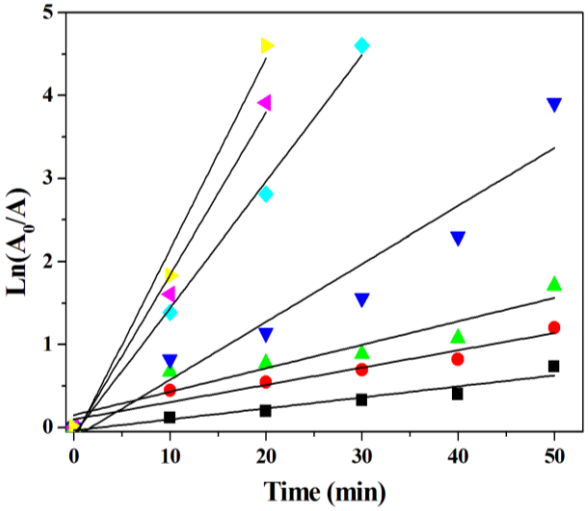

Fig. 9. Kinetics of reaction of MO dye given by ZnO nanopowders with different aluminum doped concentrations

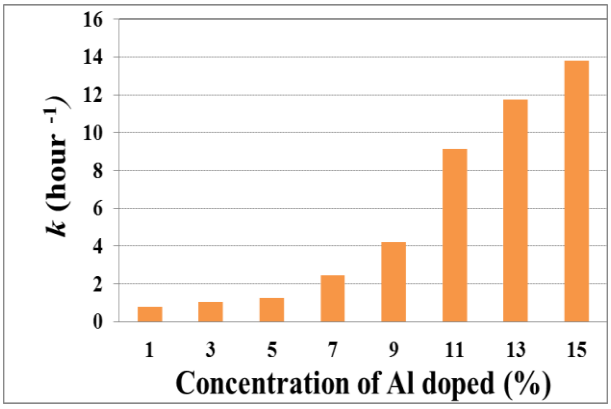

Fig. 10. Tendency of the rate of reaction obtained for the nanopowders with different aluminum doped concentrations

A simple mechanism to understand the enhancement of photocatalytic activity of ZAYO powders photocatalysts is shown in Scheme 1.According to this, the loading of Al or Y element in the ZnO lattice can accelerate the transport of photogenerated electrons to the outer systems. The Al^{3+} or Y^{3+} that incorporate in the ZnO matrix substitute zinc ions Zn^{2+} providing an extra positive charge that remains available when the photochemical reactions start; however, a charge compensation may occur making the electrons of oxygen atoms redistribute towards those positive charges, and then a negative charge is now available. Al and Y element deposited in the ZnO lattice increased the photocatalytic activity by accelerating the transfer of electrons to dissolved oxygen molecules in order to form the super-oxide radical $O2^{\bullet-}$. The holes generate OH• by reacting with the water molecules. These $O2^{\bullet-}$ radicals act as very oxidizing agents and they are also contribute to the formation of hydrogen peroxide. The formed radicals react with the MO molecule, disrupting it in its conjugated system which leads to the complete decomposition of the dye [21, 27-28].

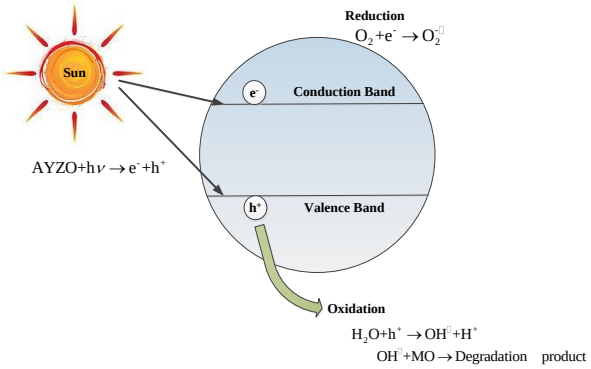

Scheme 1. A simple mechanism of photocatalytic activity of AYZO nanopowders photocatalysts

4. Conclusions

In summary, $Zn_{0.93-x}Y_{0.07}Al_xO$ (x = 0, 0.01, 0.02, and 0.03) samples were synthesized by the sol–gel method. The structural, optical and photocatalytic properties were investigated. It can be concluded that $Zn_{0.93-x}Y_{0.07}Al_xO$ samples still keep the wurtzite structure of ZnO with Al doping concentration increased, however, grain sizes decreased with Al doping concentration increased. Compared with the photocatalytic properties of samples, $Zn_{0.93-x}Y_{0.07}Al_xO$ photocatalysts show enhanced photocatalytic for MO degradation. The all samples degraded almost all the dye (about a 100%) in only 20-50 min. The doping concentration of of 15at% of Al in sample has the fastest degradation percentage, which degraded almost all the dye (about a 100%) in only 20 min. The kinetics of the reaction results exhibits the sample of 15% Al doped concentration with the highest rate (13.8 h^{-1}). In conclusion, present results indicate that Al-Y co-doped ZnO photocatalysts are potential candidate for the practical application in photocatalytic degradation of organic compounds.

Acknowledgements

The project was supported by Natural Science Basic Research Plan in Shaanxi Province of China (Program No.2015JQ2049 and No.2015JQ5144), Special Fund for Basic Scientific Research of Central Colleges, Chang'an University (No.310831151084), College Students Innovation and Entrepreneurship Training Program(No.0021-310631150521), and Applications of Environmental Friendly Materials from the Key Laboratory Ministry of Education, Jilin Normal University.

References

[1] W. L. Zhang, Y. G. Sun, D. R. Ding, P. H. Rao, L. Y. Cai, J. N. Xu, Funct. Mater. Lett. **7**, 1450052 (2014).
[2] G. Vijayaprasath, R. Murugan, G. Ravi, T. Mahalingam, Y. Hayakawa, Appl. Surf. Sci. **313**, 870 (2014).
[3] I. Novotny, S. Flickyngerova, V. Tvarozek, P. Sutta, M. Netrvalova, D. Rossberg, P. Schaaf, Appl. Surf. Sci. **312**, 167 (2014).
[4] W. M. Du, Y. P. Gao, X. Y. Zhu, Y. M. Hao, Electronic Components & Materials **33**, 35 (2014).
[5] C. Wu, W. X. Ma,Y. P. Chen, Y. Li, Y.Chen, J. Li, Applied Mechanics and Materials **482**, 34 (2014).
[6] M. A. Gondal, T. A. Saleh, Q. A. Drmosh, Appl. Surf. Sci. **258**, 6982 (2012).
[7] F. W. Kang, S. Wang,E. J. Guo, L. P. Wang, H. Y. Yue, P. Zhu, Science & Technology Review **29**, 71 (2011).
[8] H. Lei, T. Xu, C. T. Gao, J. Coat.Technol. Res. **7**, 91 (2010).
[9] Janotti, C. G. Van der Walle, Rep. Prog. Phys. **72**, 1 (2009).
[10] H. Morkoc, U. Ozgur, Materials and Device Technology, Germany, 2009.
[11] Q. Zhang, C. Dandeneau, X. Zhou, G. Cao, Adv. Mater. **21**, 1 (2009).
[12] Lupan, G. Emelchenko, V. Ursaki, G. Chai, A. Redkin, A. Gruzintsev, I. Tiginyanu, L. Chow, L. Ono, B. Cuenya, H. Heinrich, E. Yakimov, Mater. Res. Bull. **45**, 1026 (2010).
[13] M. Ohyama, H. Kozuka, T. Yoko, J. Am. Ceram. Soc. **81**, 1622 (1998).
[14] J. H. Zheng, J. L. Song, Q. Jiang, J. S. Lian, Appl. Surf. Sci. 2**58**, 6735 (2012).
[15] Y. D. Liu, J. S. Lian, Appl. Surf. Sci. **253**, 3727 (2007).
[16] H. Fu, T. Xu, S. Zhu, Y. Zhu, Environ. Sci. Technol. **42**, 8064 (2008).
[17] K. Dutta, S. Das, A. Pramanik, J. Colloid. Interf. Sci. **366**, 28 (2012).
[18] M. Bizarro, A. S. Arzate, I. G. Wilches, J. C. Alonso, A. Ortiz, Catal. Today **166**, 129 (2011).
[19] J. H. Yang, L. Y. Zhao, X. Ding, L. L. Yang, Y. J. Zhang, Y. X. Wang, H. L. Liu, Mater. Sci. Eng. B**162**, 143 (2009).
[20] F. Yakuphanoglu, J. Alloys Compd. **507**, 184 (2010).
[21] Monserrat Bizarro, Applied Catalysis B: Environmental **97**, 198 (2010).
[22] Y. Liu, J. H. Yang, Q. F. Guan, L. L.Yang, Y. J. Zhang,Y. X. Wang, B. Feng, J. Cao, X. Y. Liu, Y. T. Yang, M. B. Wei, J. Alloy. Compd. **486**, 835 (2009).
[23] C. H. Ahn, H. Kim, H. K. Cho, Thin Solid Films **519**, 747 (2010).
[24] S. Sarkar, S. Patra, S. K. Bera, G. K. Paul, R. Ghosh, Physica E **46**,1 (2012).
[25] A. A. Valenzuela, P. Russer, Appl. Phys. Lett. **55**, 1029 (1989).
[26] P. P. Sahay, R. K. Nath, Sens. Actu-ators B **134**, 654 (2008).
[27] J. M. Herrmann, Top. Catal. **34**, 49 (2005).
[28] C. A. K. Gouvea, F. Wypych, S. G. Moraes, N. Durán, N. Nagata, P. Peralta-Zamora, Chemosphere **40**, 433 (2000).

*Corresponding author: jhzheng@chd.edu.cn